Geometrically non-linear static analysis of a simply supported beam made of hyperelastic material

*T. Kocatürk and Ş.D. Akbaş[a]

*Yildiz Technical University, Davutpasa Campus, Department of Civil Engineering,
34210 Esenler-İstanbul, Turkey*

Abstract. This paper focuses on geometrically non-linear static analysis of a simply supported beam made of hyperelastic material subjected to a non-follower transversal uniformly distributed load. As it is known, the line of action of follower forces is affected by the deformation of the elastic system on which they act and therefore such forces are non-conservative. The material of the beam is assumed as isotropic and hyperelastic. Two types of simply supported beams are considered which have the following boundary conditions: 1) There is a pin at left end and a roller at right end of the beam (pinned-rolled beam). 2) Both ends of the beam are supported by pins (pinned-pinned beam). In this study, finite element model of the beam is constructed by using total Lagrangian finite element model of two dimensional continuum for a twelve-node quadratic element. The considered highly non-linear problem is solved by using incremental displacement-based finite element method in conjunction with Newton-Raphson iteration method. In order to use the solution procedures of Newton-Raphson type, there is need to linearized equilibrium equations, which can be achieved through the linearization of the principle of virtual work in its continuum form. In the study, the effect of the large deflections and rotations on the displacements and the normal stress and the shear stress distributions through the thickness of the beam is investigated in detail. It is known that in the failure analysis, the most important quantities are the principal normal stresses and the maximum shear stress. Therefore these stresses are investigated in detail. The convergence studies are performed for various numbers of finite elements. The effects of the geometric non-linearity and pinned-pinned and pinned-rolled support conditions on the displacements and on the stresses are investigated. By using a twelve-node quadratic element, the free boundary conditions are satisfied and very good stress diagrams are obtained. Also, some of the results of the total Lagrangian finite element model of two dimensional continuum for a twelve-node quadratic element are compared with the results of SAP2000 packet program. Numerical results show that geometrical nonlinearity plays very important role in the static responses of the beam.

Keywords: geometrical non-linearity; simply supported beams; finite element analysis; total lagrangian finite element model; two dimensional solid continuum.

1. Introduction

With the great advances in technology in recent years, increasing demands for higher operational speeds and lighter device constructions makes it necessary to use non-linear theory of beams. For

---

*Corresponding author, Professor, E-mail: kocaturk@yildiz.edu.tr
[a]Research Assistant

example, the deflections of a leaf spring used in ground vehicles must be studied by using non-linear theory of beams. In the past 50 years, especially, developments in aerospace engineering, robotics and manufacturing make it inevitable to excessively use non-linear models that must be solved numerically. Because, closed-form solutions of large-deflection problems of beams with general loading and boundary conditions using elliptic integrals are limited. Some of these studies concerning closed-form solutions are given in the following paragraphs: Chucheepsakul *et al*. (1994) studied the large deflections of beams under moment gradients whose deformed arc lengths are not fixed by using the elliptic integral method, the shooting-optimization method and the finite element method. Pulngern *et al*. (2005) investigated large static deflection due to uniformly distributed self weight and the critical or maximum applied uniform loading that a simply supported beam with variable-arc-length can resist by using both finite-element method discretization of the span length based on variational formulation and shooting method based on an elastic theory formulation. Al Sadder *et al*. (2006) developed an improved finite element formulation with a scheme of solution for the large deflection analysis of inextensible prismatic and nonprismatic slender beams. Wang *et al*. (1997) considered the large deflection problem of variable deformed arc-length beams considering one end of the beam being hinged and the beam being allowed to slide freely on a frictionless support located at a specified distance away from this hinged end under a point load. A similar problem was solved by He *et al*. (1997) in which only the frictionless support in the previous study was assumed as a friction support. Some of the numerical studies are given in the following paragraphs: Kapania and Li (2003) formulated and implemented exact curved beam elements incorporating finite strains and finite rotations. Al Sadder and Al Rawi (2006) developed a quasi-linearization finite differences scheme for large deflection analysis of prismatic and non-prismatic slender cantilever beams subjected to various types of continuous and discontinuous external variable distributed and concentrated loads in horizontal and vertical global directions. Li and Zhou (2005) investigated the post-buckling behavior of a hinged-fixed beam under uniformly distributed follower forces by deriving an exact mathematical model and using the shooting method for numerical results. Large deflection static analysis of simple beams was investigated by Akbaş and Kocatürk (2009). Geometrically nonlinear analysis of a cantilever beam was investigated by Reddy (2004) by using an eight-node quadratic element.

The aim of this paper is to compute the displacements of the considered simply supported beams made of hyperelastic material.

As it is known, when two dimensions of a structural element is very small compared to the other dimension, then, for reducing the number of unknowns, one of the beam theories is used. When the dimensions of the considered element become close to each other, the beam theories lose accuracy and therefore they are not valid any more. According to assumptions made in these theories, some of the free boundary conditions can not be satisfied. However, in two dimensional solid continuum assumption, only one dimension of the considered element is small compared to other dimensions. In the present study, every finite element of the beam is assumed as a two dimensional solid continuum. Therefore, it is necessary to satisfy free boundary conditions. Satisfying the free boundary conditions and obtaining smooth stress distributions in the finite element analysis of two dimensional solid continuum is not an easy task. It is more troublesome when dealing with nonlinear problems. In this study, free boundary conditions are satisfied satisfactorily and smooth stress diagrams are obtained by choosing a twelve-node quadratic element.

The development of the formulations of general solution procedure of nonlinear problems follows the general outline of the derivation given by Zienkiewichz and Taylor (2000). The geometrically

non-linear responses of considered simply supported beams subjected to a non-follower transversal uniformly distributed load are obtained by using total Lagrangian finite element model of two-dimensional solid continuum. The TL finite element equations of two dimensional continuum for a twelve-node quadratic element are used. These TL twelve-node quadratic element formulations were given by Reddy (2004). Convergence studies are performed for various numbers of elements.

2. Theory and formulations

Two simply supported beams made of isotropic, hyperelastic material, with material or Lagrangian coordinate system ($^0x_1$, $^0x_2$, $^0x_3$) and with spatial or Euler coordinate system ($^2x_1$, $^2x_2$, $^2x_3$) having the origin *O is* shown in Figs. 1(a),(b).

One of the supports of the beam is assumed to be pinned and the other is a roller. The beam is subjected to a uniformly distributed non-follower load in the transverse direction as seen from Fig. 1.

While the derivation of the governing equations for most problems is not unduly difficult, their solution by exact methods of analysis is a formidable task. In such cases, numerical methods of analysis provide an alternative means of finding solutions. Numerical methods typically transform differential equations to algebraic equations that are to be solved using computers. The considered problem is a nonlinear one. Even linear problems may not admit exact solutions due to geometric and material complexities, but it is relatively easy to obtain approximate solutions using numerical methods (Reddy 2004). There are some solutions for the special cases of boundary and loading conditions for large displacements of beams in the framework of Bernoulli-Euler beam theory. However, as far as the authors know exact solution of a nonlinear problem in the framework of two or three-dimensional continuum approach is not possible. For the analysis of the simply supported beam, the beam problem is considered as a two-dimensional continua problem: The total Lagrangian Finite element model of two dimensional continuum based on the total Lagrangian formulation for a twelve-node quadratic element is used in the study. For the solution of the total Lagrangian formulations of TL two dimensional continuum problem, small-step incremental approaches from known solutions are used. As it is known, it is possible to obtain solutions in a single increment of the external force only in the case of mild nonlinearity (and no path dependence). To obtain realistic answers, physical insight into the nature of the problem and, usually, small-step incremental approaches
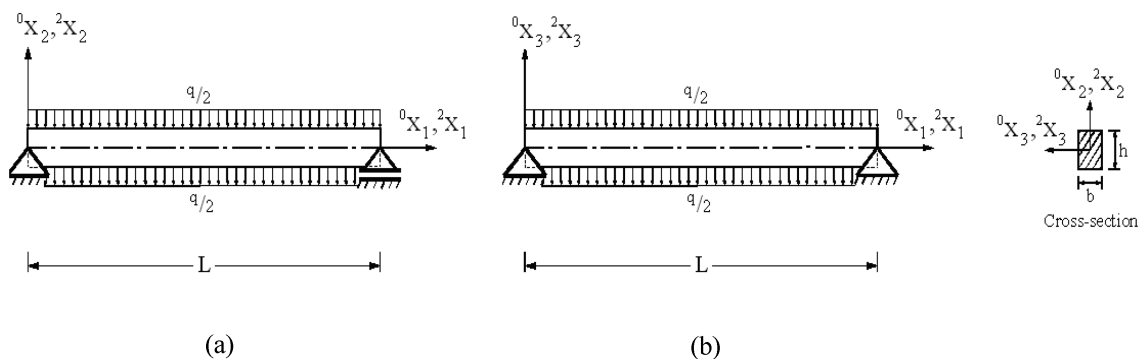

Fig. 1 Simply supported beam subjected to a uniformly distributed load (a) pinned-rolled beam, (b) pinned-pinned beam

from known solutions are essential. Such increments are always required if the constitutive law relating stress and strain changes is path dependent. Also, such incremental procedures are useful to reduce excessive numbers of iterations and in following the physically correct path.

In this study, small-step incremental approaches from known solutions with Newton-Raphson iteration method are used in which the solution for $n+1$th load increment and ith iteration is obtained in the following form

$$d\mathbf{u}_n^i = (\mathbf{K}_T^i)^{-1}\mathbf{R}_{n+1}^i \tag{1}$$

Where $\mathbf{K}_T^i$ is the stiffness matrix corresponding to a tangent direction at the ith iteration, $d\mathbf{u}_n^i$ is the solution increment vector at the ith iteration and $n+1$th load increment, $\mathbf{R}_{n+1}^i$ is the residual vector at the ith iteration and $n+1$th load increment. This iteration procedure is continued until the difference between two successive solution vectors is less than a selected tolerance criterion in Euclidean norm given by

$$\sqrt{\frac{[(d\mathbf{u}_n^{i+1} - d\mathbf{u}_n^i)^T(d\mathbf{u}_n^{i+1} - d\mathbf{u}_n^i)]^2}{[(d\mathbf{u}_n^{i+1})^T(d\mathbf{u}_n^{i+1})]^2}} \leq \zeta_{tol} \tag{2}$$

A series of successive approximations gives

$$\mathbf{u}_{n+1}^{i+1} = \mathbf{u}_{n+1}^i + d\mathbf{u}_{n+1}^i = \mathbf{u}_n + \Delta\mathbf{u}_n^i \tag{3}$$

where

$$\Delta\mathbf{u}_n^i = \sum_{k=1}^i d\mathbf{u}_n^k \tag{4}$$

The tangent stiffness matrix $\mathbf{K}_T^i$ and the residual vector $\mathbf{R}_{n+1}^i$ which are to be used in Eq. (1) at the ith iteration for the total Lagrangian finite element model of two dimensional continuum for a twelve-node quadratic element are given below

$$\begin{bmatrix} \mathbf{K}^{11L} + \mathbf{K}^{11NL} & \mathbf{K}^{12L} \\ \mathbf{K}^{21L} & \mathbf{K}^{22L} + \mathbf{K}^{22NL} \end{bmatrix}^i \begin{Bmatrix} \bar{\mathbf{u}} \\ \bar{\mathbf{v}} \end{Bmatrix}^i = \begin{Bmatrix} {}_0^2\mathbf{F}^1 - {}_0^1\mathbf{F}^1 \\ {}_0^2\mathbf{F}^2 - {}_0^1\mathbf{F}^2 \end{Bmatrix}^i \tag{5}$$
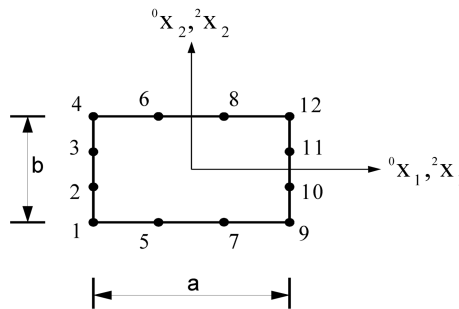

Fig. 2 A twelve-node quadratic plane element

where

$$K_{ij}^{11L} = h_e \int_{\Omega^e} \left\{ {}_0C_{11} \left(1 + \frac{\partial u}{\partial\, {}^0x_1} \right)^2 \frac{\partial\psi_i}{\partial\, {}^0x_1} \frac{\partial\psi_j}{\partial\, {}^0x_1} + {}_0C_{22} \left(\frac{\partial u}{\partial\, {}^0x_2} \right)^2 \frac{\partial\psi_i}{\partial\, {}^0x_2} \frac{\partial\psi_j}{\partial\, {}^0x_2} \right.$$

$$+ {}_0C_{12} \left(1 + \frac{\partial u}{\partial\, {}^0x_1} \right) \frac{\partial u}{\partial\, {}^0x_2} \left(\frac{\partial\psi_i}{\partial\, {}^0x_1} \frac{\partial\psi_j}{\partial\, {}^0x_1} + \frac{\partial\psi_i}{\partial\, {}^0x_2} \frac{\partial\psi_j}{\partial\, {}^0x_1} \right)$$

$$+ {}_0C_{66} \left[\left(1 + \frac{\partial u}{\partial\, {}^0x_1} \right) \frac{\partial\psi_i}{\partial\, {}^0x_2} + \frac{\partial u}{\partial\, {}^0x_2} \frac{\partial\psi_i}{\partial\, {}^0x_1} \right] \times \left. \left[\left(1 + \frac{\partial u}{\partial\, {}^0x_1} \right) \frac{\partial\psi_j}{\partial\, {}^0x_2} + \frac{\partial u}{\partial\, {}^0x_2} \frac{\partial\psi_j}{\partial\, {}^0x_1} \right] \right\} d\, {}^0x_1 d\, {}^0x_2 \qquad (6a)$$

$$K_{ij}^{12L} = h_e \int_{\Omega^e} \left\{ {}_0C_{11} \left(1 + \frac{\partial u}{\partial\, {}^0x_1} \right) \frac{\partial v}{\partial\, {}^0x_1} \frac{\partial\psi_i}{\partial\, {}^0x_1} \frac{\partial\psi_j}{\partial\, {}^0x_1} + {}_0C_{22} \left(1 + \frac{\partial v}{\partial\, {}^0x_2} \right) \frac{\partial u}{\partial\, {}^0x_2} \frac{\partial\psi_i}{\partial\, {}^0x_2} \frac{\partial\psi_j}{\partial\, {}^0x_2} \right.$$

$$+ {}_0C_{12} \left[\left(1 + \frac{\partial u}{\partial\, {}^0x_1} \right)\left(1 + \frac{\partial v}{\partial\, {}^0x_2} \right) \frac{\partial\psi_i}{\partial\, {}^0x_1} \frac{\partial\psi_j}{\partial\, {}^0x_2} + \frac{\partial u}{\partial\, {}^0x_2} \frac{\partial v}{\partial\, {}^0x_1} \frac{\partial\psi_i}{\partial\, {}^0x_2} \frac{\partial\psi_j}{\partial\, {}^0x_1} \right]$$

$$+ {}_0C_{66} \left[\left(1 + \frac{\partial u}{\partial\, {}^0x_1} \right) \frac{\partial\psi_i}{\partial\, {}^0x_2} + \frac{\partial u}{\partial\, {}^0x_2} \frac{\partial\psi_i}{\partial\, {}^0x_1} \right] \times \left. \left[\left(1 + \frac{\partial v}{\partial\, {}^0x_2} \right) \frac{\partial\psi_j}{\partial\, {}^0x_1} + \frac{\partial v}{\partial\, {}^0x_1} \frac{\partial\psi_j}{\partial\, {}^0x_2} \right] \right\} d^0x_1 d^0x_2 = K_{ji}^{21L} \quad (6b)$$

$$K_{ij}^{22L} = h_e \int_{\Omega^e} \left\{ {}_0C_{11} \left(\frac{\partial v}{\partial\, {}^0x_1} \right)^2 \frac{\partial\psi_i}{\partial\, {}^0x_1} \frac{\partial\psi_j}{\partial\, {}^0x_1} + {}_0C_{22} \left(1 + \frac{\partial v}{\partial\, {}^0x_2} \right)^2 \frac{\partial\psi_i}{\partial\, {}^0x_2} \frac{\partial\psi_j}{\partial\, {}^0x_2} \right.$$

$$+ {}_0C_{12} \left(1 + \frac{\partial v}{\partial\, {}^0x_2} \right) \frac{\partial v}{\partial\, {}^0x_1} \left(\frac{\partial\psi_i}{\partial\, {}^0x_1} \frac{\partial\psi_j}{\partial\, {}^0x_2} + \frac{\partial\psi_i}{\partial\, {}^0x_2} \frac{\partial\psi_j}{\partial\, {}^0x_1} \right)$$

$$+ {}_0C_{66} \left[\left(1 + \frac{\partial v}{\partial\, {}^0x_2} \right) \frac{\partial\psi_i}{\partial\, {}^0x_1} + \frac{\partial v}{\partial\, {}^0x_1} \frac{\partial\psi_i}{\partial\, {}^0x_2} \right] \times \left. \left[\left(1 + \frac{\partial v}{\partial\, {}^0x_2} \right) \frac{\partial\psi_j}{\partial\, {}^0x_1} + \frac{\partial v}{\partial\, {}^0x_1} \frac{\partial\psi_j}{\partial\, {}^0x_2} \right] \right\} d^0x_1 d^0x_2 \qquad (6c)$$

$$K_{ij}^{11NL} = h_e \int_{\Omega^e} \left[{}_0^1S_{11} \frac{\partial\psi_i}{\partial\, {}^0x_1} \frac{\partial\psi_j}{\partial\, {}^0x_1} + {}_0^1S_{12} \left(\frac{\partial\psi_i}{\partial\, {}^0x_2} \frac{\partial\psi_j}{\partial\, {}^0x_1} + \frac{\partial\psi_i}{\partial\, {}^0x_1} \frac{\partial\psi_j}{\partial\, {}^0x_2} \right) \right.$$

$$\left. + {}_0^1S_{22} \frac{\partial\psi_i}{\partial\, {}^0x_2} \frac{\partial\psi_j}{\partial\, {}^0x_2} \right] d^0x_1 d^0x_1 = K_{ij}^{22N} \qquad (6d)$$

$${}_0^2F_i^1 = h_e \int_{\Omega^e} {}_0^2 f_{{}_0x_1} \psi_i d^0x_1 d^0x_1 + h_e \int_{\Gamma^e} {}_0^2 t_{{}_0x_1} \psi_i d^0x_1 \qquad (6e)$$

$${}_0^2F_i^2 = h_e \int_{\Omega^e} {}_0^2 f_{{}_0x_2} \psi_i d^0x_1 d^0x_2 + h_e \int_{\Gamma^e} {}_0^2 t_{{}_0x_2} \psi_i d^0x_1 \qquad (6f)$$

where ${}_0^2 f_{{}_0x_1}$, ${}_0^2 f_{{}_0x_1}$ are the body forces, ${}_0^2 t_{{}_0x_1}$, ${}_0^2 t_{{}_0x_2}$ are the surface forces in the ${}^0x_1$ and ${}^0x_2$ directions.

$$
{}_0^1F_i^1 = h_e \int_{\Omega^e} \left\{ \left(1 + \frac{\partial u}{\partial {}^0x_1}\right)\frac{\partial \psi_i}{\partial {}^0x_1}{}_0^1S_{11} + \frac{\partial u}{\partial {}^0x_2}\frac{\partial \psi_i}{\partial {}^0x_2}{}_0^1S_{22} \right.
$$

$$
\left. + \left[\left(1 + \frac{\partial u}{\partial {}^0x_1}\right)\frac{\partial \psi_i}{\partial {}^0x_2} + \frac{\partial u}{\partial {}^0x_2}\frac{\partial \psi_i}{\partial {}^0x_1}\right]{}_0^1S_{12} \right\} d^0x_1 d^0x_1 \tag{7}
$$

$$
{}_0^1F_i^2 = h_e \int_{\Omega^e} \left\{ \frac{\partial v}{\partial {}^0x_1}\frac{\partial \psi_i}{\partial {}^0x_1}{}_0^1S_{11} + \left(1 + \frac{\partial v}{\partial {}^0x_2}\right)\frac{\partial \psi_i}{\partial {}^0x_2}{}_0^1S_{22} \right.
$$

$$
\left. + \left[\left(1 + \frac{\partial v}{\partial {}^0x_2}\right)\frac{\partial \psi_i}{\partial {}^0x_1} + \frac{\partial v}{\partial {}^0x_1}\frac{\partial \psi_i}{\partial {}^0x_2}\right]{}_0^1S_{12} \right\} d^0x_1 d^0x_2 \tag{8}
$$

where ${}_0^1S_{11}$, ${}_0^1S_{22}$, ${}_0^1S_{12}$ are the components of the second Piola-Kirchhoff stress tensor components in the C_1 configuration of the body. The considered material is hyperelastic. In this case, the constitutive relation between the second Piola-Kirchhoff stress tensor (Transformed current force per unit undeformed area: This tensor is symmetric whenever the Cauchy stress tensor is symmetric.) and the Green-Lagrange strain tensor can be assumed as follows

$$
{}_0^1\mathbf{S} = \begin{Bmatrix} {}_0^1S_{11} \\ {}_0^1S_{22} \\ {}_0^1S_{12} \end{Bmatrix} = \begin{bmatrix} {}_0C_{11} & {}_0C_{12} & 0 \\ {}_0C_{12} & {}_0C_{22} & 0 \\ 0 & 0 & {}_0C_{66} \end{bmatrix} \begin{Bmatrix} {}_0^1E_{11} \\ {}_0^1E_{22} \\ 2{}_0^1E_{12} \end{Bmatrix} \tag{9}
$$

Where ${}_0C_{ij}$ are the components of the reduced constitutive tensor in the C_0 configuration of the body. The reduced constitutive tensor can be written in the matrix form as follows

$$
{}_0\mathbf{C} = \begin{bmatrix} {}_0C_{11} & {}_0C_{12} & 0 \\ {}_0C_{12} & {}_0C_{22} & 0 \\ 0 & 0 & {}_0C_{66} \end{bmatrix} \tag{10}
$$

Where the components of the reduced constitutive tensor can be written in terms of Young modulus E and Poisson's ratio v as follows

$$
{}_0C_{11} = \frac{E}{1-v^2}, \quad {}_0C_{12} = {}_0C_{21} = \frac{vE}{1-v^2}, \quad {}_0C_{22} = \frac{E}{1-v^2}, \quad {}_0C_{66} = \frac{E}{2(1+v)} \tag{11}
$$

The Green-Lagrange strain tensor is expressed in terms of displacements in the case of two-dimensional solid continuum as follows

$$
{}_0^1\mathbf{E} = \begin{Bmatrix} {}_0^1E_{11} \\ {}_0^1E_{22} \\ 2{}_0^1E_{12} \end{Bmatrix} = \begin{Bmatrix} \dfrac{\partial u}{\partial {}^0x_1} + \dfrac{1}{2}\left[\left(\dfrac{\partial u}{\partial {}^0x_1}\right)^2 + \left(\dfrac{\partial v}{\partial {}^0x_1}\right)^2\right] \\[12pt] \dfrac{\partial v}{\partial {}^0x_2} + \dfrac{1}{2}\left[\left(\dfrac{\partial u}{\partial {}^0x_2}\right)^2 + \left(\dfrac{\partial v}{\partial {}^0x_2}\right)^2\right] \\[12pt] \dfrac{\partial u}{\partial {}^0x_2} + \dfrac{\partial v}{\partial {}^0x_1} + \left(\dfrac{\partial u}{\partial {}^0x_1}\dfrac{\partial u}{\partial {}^0x_2} + \dfrac{\partial v}{\partial {}^0x_1}\dfrac{\partial v}{\partial {}^0x_2}\right) \end{Bmatrix} \tag{12}
$$

where the displacement fields of the finite element are expressed in terms of nodal displacements as follows

$$u = (\psi_1 \cdot u_1 + \psi_2 \cdot u_2 + \psi_3 \cdot u_3 + \psi_4 \cdot u_4 + \psi_5 \cdot u_5 + \psi_6 \cdot u_6 + \psi_7 \cdot u_7 + \psi_8 \cdot u_8 + \psi_9 \cdot u_9 + \psi_{10} \cdot u_{10}$$
$$+ \psi_{11} \cdot u_{11} + \psi_{12} \cdot u_{12}) \tag{13}$$

$$v = (\psi_1 \cdot v_1 + \psi_2 \cdot v_2 + \psi_3 \cdot v_3 + \psi_4 \cdot v_4 + \psi_5 \cdot v_5 + \psi_6 \cdot v_6 + \psi_7 \cdot v_7 + \psi_8 \cdot v_8 + \psi_9 \cdot v_9 + \psi_{10} \cdot v_{10}$$
$$+ \psi_{11} \cdot v_{11} + \psi_{12} \cdot v_{12}) \tag{14}$$

These total displacement fields and incremental displacement fields are interpolated as follows

$$\{u\} = \begin{Bmatrix} u \\ v \end{Bmatrix} = \begin{Bmatrix} \sum_{j=1}^{12} u_j \psi_j(^ox_1, {}^ox_2) \\ \sum_{j=1}^{12} v_j \psi_j(^ox_1, {}^ox_2) \end{Bmatrix} = [\Psi]\{\Delta\} \tag{15a}$$

$$\{\bar{u}\} = \begin{Bmatrix} \bar{u} \\ \bar{v} \end{Bmatrix} = \begin{Bmatrix} \sum_{j=1}^{12} \bar{u}_j \psi_j(^ox_1, {}^ox_2) \\ \sum_{j=1}^{12} \bar{v}_j \psi_j(^ox_1, {}^ox_2) \end{Bmatrix} = [\Psi]\{du\} \tag{15b}$$

where

$$[\psi] = \begin{bmatrix} \psi_1 & 0 & \psi_2 & 0 & \psi_3 & 0 & \psi_4 & 0 & \psi_5 & 0 & \psi_6 & 0 & \psi_7 & 0 & \psi_8 & 0 & \psi_9 & 0 & \psi_{10} & 0 & \psi_{11} & 0 & \psi_{12} & 0 \\ 0 & \psi_1 & 0 & \psi_2 & 0 & \psi_3 & 0 & \psi_4 & 0 & \psi_5 & 0 & \psi_6 & 0 & \psi_7 & 0 & \psi_8 & 0 & \psi_9 & 0 & \psi_{10} & 0 & \psi_{11} & 0 & \psi_{12} \end{bmatrix} \tag{16}$$

$$\{\Delta\}^T = \{u_1 \ v_1 \ u_2 \ v_2 \ u_3 \ v_3 \ u_4 \ v_4 \ u_5 \ v_5 \ u_6 \ v_6 \ u_7 \ v_7 \ u_8 \ v_8 \ u_9 \ v_9 \ u_{10} \ v_{10} \ u_{11} \ v_{11} \ u_{12} \ v_{12}\} \tag{17}$$

$$\{du\}^T = \{\bar{u}_1 \ \bar{v}_1 \ \bar{u}_2 \ \bar{v}_2 \ \bar{u}_3 \ \bar{v}_3 \ \bar{u}_4 \ \bar{v}_4 \ \bar{u}_5 \ \bar{v}_5 \ \bar{u}_6 \ \bar{v}_6 \ \bar{u}_7 \ \bar{v}_7 \ \bar{u}_8 \ \bar{v}_8 \ \bar{u}_9 \ \bar{v}_9 \ \bar{u}_{10} \ \bar{v}_{10} \ \bar{u}_{11} \ \bar{v}_{11} \ \bar{u}_{12} \ \bar{v}_{12}\} \tag{18}$$

Interpolation functions for a twelve-node quadratic element are as follows

$$[\psi_1] = \frac{1}{32}\left(1 - \frac{2\,{}^0x_1}{a}\right)\left(1 - \frac{2\,{}^0x_2}{b}\right)\left(-10 + 9\left(\frac{4\,{}^0x_1^2}{a^2} + \frac{4\,{}^0x_2^2}{b^2}\right)\right)$$

$$[\psi_2] = \frac{9}{32}\left(1 - \frac{2\,{}^0x_1}{a}\right)\left(1 - \frac{4\,{}^0x_2^2}{b^2}\right)\left(1 - \frac{6\,{}^0x_2}{b}\right)$$

$$[\psi_3] = \frac{9}{32}\left(1 - \frac{2\,{}^0x_1}{a}\right)\left(1 - \frac{4\,{}^0x_2^2}{b^2}\right)\left(1 + \frac{6\,{}^0x_2}{b}\right)$$

$$[\psi_4] = \frac{1}{32}\left(1 - \frac{2\,{}^0x_1}{a}\right)\left(1 + \frac{2\,{}^0x_2}{b}\right)\left(-10 + 9\left(\frac{4\,{}^0x_1^2}{a^2} + \frac{4\,{}^0x_2^2}{b^2}\right)\right)$$

$$[\psi_5] = \frac{9}{32}\left(1 - \frac{2\,^0x_2}{b}\right)\left(1 - \frac{4\,^0x_1^2}{a^2}\right)\left(1 - \frac{6\,^0x_1}{a}\right)$$

$$[\psi_6] = \frac{9}{32}\left(1 + \frac{2\,^0x_2}{b}\right)\left(1 - \frac{4\,^0x_1^2}{a^2}\right)\left(1 - \frac{6\,^0x_1}{a}\right)$$

$$[\psi_7] = \frac{9}{32}\left(1 - \frac{2\,^0x_2}{b}\right)\left(1 - \frac{4\,^0x_1^2}{a^2}\right)\left(1 + \frac{6\,^0x_1}{a}\right)$$

$$[\psi_8] = \frac{9}{32}\left(1 + \frac{2\,^0x_2}{b}\right)\left(1 - \frac{4\,^0x_1^2}{a^2}\right)\left(1 + \frac{6\,^0x_1}{a}\right)$$

$$[\psi_9] = \frac{1}{32}\left(1 + \frac{2\,^0x_1}{a}\right)\left(1 - \frac{2\,^0x_2}{b}\right)\left(-10 + 9\left(\frac{4\,^0x_1^2}{a^2} + \frac{4\,^0x_2^2}{b^2}\right)\right)$$

$$[\psi_{10}] = \frac{9}{32}\left(1 + \frac{2\,^0x_1}{a}\right)\left(1 - \frac{4\,^0x_2^2}{b^2}\right)\left(1 - \frac{6\,^0x_2}{b}\right)$$

$$[\psi_{11}] = \frac{9}{32}\left(1 + \frac{2\,^0x_1}{a}\right)\left(1 - \frac{4\,^0x_2^2}{b^2}\right)\left(1 + \frac{6\,^0x_2}{b}\right)$$

$$[\psi_{12}] = \frac{1}{32}\left(1 + \frac{2\,^0x_1}{a}\right)\left(1 + \frac{2\,^0x_2}{b}\right)\left(-10 + 9\left(\frac{4\,^0x_1^2}{a^2} + \frac{4\,^0x_2^2}{b^2}\right)\right) \tag{19}$$

Numerical calculations of the integral seen in the rigidity matrices will be calculated by using five-point Gauss rule.

The true stress, namely stress in the deformed configuration is defined to be the current force per unit deformed area. The relation between the Cauchy stress tensor components $^2\sigma_{ij}$ and the second Piola-Kirchhoff stress tensor components $^2_0S_{ij}$ can be written as follows

$$^2\sigma_{ij} = \frac{^2\rho}{^0\rho}\frac{\partial^2 x_i}{\partial^0 x_p}\frac{\partial^2 x_j}{\partial^0 x_q}\,^2_0S_{pq} \tag{20}$$

Where $^0\rho$ and $^2\rho$ represent the mass densities of the material in configurations C_0 and C_2 respectively. The relation between the $^0\rho$ and $^2\rho$ is as follows

$$^0\rho = \,^2\rho\,^2_0J \tag{21}$$

Where ^2_0J is the determinant of the deformation gradient tensor $^2_0\mathbf{F}$ (or the Jacobian of the transformation) and defined as follows

$$^2_0J = \det(^2_0\mathbf{F}) = \left|\frac{\partial^2 x_i}{\partial^0 x_j}\right| = \begin{vmatrix} \dfrac{\partial^2 x_1}{\partial^0 x_1} & \dfrac{\partial^2 x_1}{\partial^0 x_2} & \dfrac{\partial^2 x_1}{\partial^0 x_3} \\[2ex] \dfrac{\partial^2 x_2}{\partial^0 x_1} & \dfrac{\partial^2 x_2}{\partial^0 x_2} & \dfrac{\partial^2 x_2}{\partial^0 x_3} \\[2ex] \dfrac{\partial^2 x_3}{\partial^0 x_1} & \dfrac{\partial^2 x_3}{\partial^0 x_2} & \dfrac{\partial^2 x_3}{\partial^0 x_3} \end{vmatrix} \tag{22}$$

The following transformation rule hold between the components of the elasticity tensors in different configurations

$$_{2}C_{ijkl} = \frac{^{2}\rho}{_{0}\rho} \frac{\partial^{2}x_{i}}{\partial^{0}x_{p}} \frac{\partial^{2}x_{j}}{\partial^{0}x_{q}} \frac{\partial^{2}x_{k}}{\partial^{0}x_{r}} \frac{\partial^{2}x_{l}}{\partial^{0}x_{s}} {}_{0}C_{pqrs} \tag{23}$$

It is assumed in the study that the components of the reduced constitutive tensor remain constant during the deformation. Namely, it is assumed that $_{0}\rho \approx {}_{2}\rho$ and therefore $_{0}C_{ij} = {}_{2}C_{ij}$. The error introduced by this assumption can be negligible if the strains are relatively small but the difference can be significant in large deformation problems.

The total displacements of a particle in the two configurations C_0 and C_2 can be written as

$$_{0}^{2}u_{i} = {}^{2}x_{i} - {}^{0}x_{i} \tag{24}$$

From Eq. (23), the relation between $^{2}x_{i}$ and $^{0}x_{i}$ can be written as follows

$$^{2}x_{i} = {}^{0}x_{i} + {}_{0}^{2}u_{i} \tag{25}$$

A material line $d\mathbf{L}$ before deformation deforms to the line $d\mathbf{l}$ (consisting of the same material as $d\mathbf{L}$) after deformation as follows

$$d\mathbf{l} = {}_{0}^{2}\mathbf{F} d\mathbf{L} \tag{26}$$

where

$$_{0}^{2}\mathbf{F} = F_{ij} {}^{0}\mathbf{e}_{i} {}^{2}\mathbf{e}_{j}, \quad F_{ij} = \frac{\partial^{2}x_{i}}{\partial^{0}x_{j}} \tag{27}$$

or more explicitly

$$[F] = \begin{vmatrix} \dfrac{\partial^{2}x_{1}}{\partial^{0}x_{1}} & \dfrac{\partial^{2}x_{1}}{\partial^{0}x_{2}} & \dfrac{\partial^{2}x_{1}}{\partial^{0}x_{3}} \\[2mm] \dfrac{\partial^{2}x_{2}}{\partial^{0}x_{1}} & \dfrac{\partial^{2}x_{2}}{\partial^{0}x_{2}} & \dfrac{\partial^{2}x_{2}}{\partial^{0}x_{3}} \\[2mm] \dfrac{\partial^{2}x_{3}}{\partial^{0}x_{1}} & \dfrac{\partial^{2}x_{3}}{\partial^{0}x_{2}} & \dfrac{\partial^{2}x_{3}}{\partial^{0}x_{3}} \end{vmatrix} \tag{28}$$

The formulations given by Eqs. (5) to (28) are adopted from Reddy (2004).

3. Solution of the system of equilibrium equations and numerical results

By use of usual assembly process, the system tangent stiffness matrix given in Eq. (1) is obtained by using the element stiffness matrixes given above for the total Lagrangian Finite element model of two dimensional continuum based on the total Lagrangian formulation for a twelve-node quadratic element. In the numerical integrations, five-point Gauss integration rule is used. Length of the beam is $L = 16$ cm, 20 cm, 30 cm, 40 cm, 50 cm, width of the beam is $b = 1$ cm and height of the beam is $h = 2$ cm. In the numerical analysis, Young's modulus is taken as $E = 8300$ N/cm^2 and

Poisson's ratio is taken as $v = 0.2$ for the hyperelastic material. Convergence analysis is performed for external distributed load $q = 70$ N/cm^2 for various numbers of finite elements in ${}^0x_1$ and ${}^0x_2$ directions when $L/h = 8$. It is seen from Table 1(a) and Figs. 3 and 4 that, when the number of finite elements in ${}^0x_1$ direction is $m = 35$ and when the number of elements in ${}^0x_2$ direction is $n = 6$ for the total Lagrangian finite element model of two dimensional continuum for a twelve-node quadratic element, the considered stresses and displacements converge perfectly. It is seen from Table 1(b) that when the number of finite elements in ${}^0x_1$ direction is $m = 70$ for the SAP2000 solution of the problem, the considered displacements converge perfectly. Therefore, in the numerical calculations, the number of finite elements in ${}^0x_1$ direction is taken as $m = 35$ and the number of elements in ${}^0x_2$ direction is taken as $n = 6$ for the total Lagrangian finite element model of two dimensional continua. For the SAP2000 analysis, the number of elements in ${}^0x_1$ direction is taken as $m = 70$. Note also that all the computations of the total Lagrangian finite element model of two dimensional continuum are performed in-house.

Fig. 5 shows that increase in load causes increase in difference between the vertical displacement values of the linear and the nonlinear solutions and also between the displacement values of the finite element model of two dimensional continuum and SAP2000 for geometrically nonlinear case.

Table 1(a) Convergence analysis of finite element model of two dimensional continuum for pinned-rolled beam for stresses in ${}^0x_1 = 8$ cm, ${}^0x_2 = 0.0$ cm and for displacements in ${}^0x_1 = 8$ cm, ${}^0x_2 = 0.0$ cm (at the middle of the beam) for distributed load $q = 70$ N/cm^2, beam length $L = 16$ cm. m: number of elements in ${}^0x_1$ direction, n: number of elements in ${}^0x_2$ direction

m	n	Stresses (N/cm^2)			Deflection (cm)		
		${}^2\sigma_{11}$	${}^2\sigma_{22}$	${}^2\sigma_{12}$	u (8; 0)	v (8; 0)	u (16; 0)
15	2	-238.0111	-263.3170	0	-2.6711	-5.3997	-5.3421
	4	-239.8984	-264.7628	0	-2.6710	-5.4065	-5.3420
	6	-240.1717	-265.5260	0	-2.6710	-5.4130	-5.3420
	8	-240.2631	-265.8356	0	-2.6710	-5.4161	-5.3420
20	2	-239.2291	-264.1622	0	-2.6711	-5.4078	-5.3422
	4	-240.4986	-265.5659	0	-2.6710	-5.4131	-5.3420
	6	-240.6484	-266.0938	0	-2.6710	-5.4178	-5.3420
	8	-240.7618	-266.3642	0	-2.6710	-5.4192	-5.3420
25	2	-240.0188	-264.7759	0	-2.6711	-5.4117	-5.3422
	4	-240.8388	-266.1170	0	-2.6710	-5.4155	-5.3420
	6	-240.8946	-266.4585	0	-2.6710	-5.4197	-5.3420
	8	-240.9302	-266.5015	0	-2.6710	-5.4209	-5.3420
30	2	-240.2818	-264.9948	0	-2.6711	-5.4139	-5.3422
	4	-240.9477	-266.3192	0	-2.6710	-5.4176	-5.3420
	6	-240.9682	-266.5891	0	-2.6710	-5.4214	-5.3420
	8	-241.0126	-266.6012	0	-2.6710	-5.4218	-5.3420
35	2	-240.5084	-265.1899	0	-2.6711	-5.4153	-5.3422
	4	-241.0446	-266.5104	0	-2.6710	-5.4187	-5.3420
	6	-241.0686	-266.6197	0	-2.6710	-5.4219	-5.3420
	8	-241.0702	-266.6263	0	-2.6710	-5.4221	-5.3420

Table 1(b) Convergence analysis of SAP2000 solution for pinned-rolled beam for stresses in $^0x_1 = 8$ cm, $^0x_2 = 0.0$ cm and for displacements in $^0x_1 = 8$ cm, $^0x_2 = 0.0$ cm (at the middle of the beam) for distributed load $q = 70$ N/cm^2, beam length $L = 16$ cm. m: number of elements in $^0x_1$ direction

m	Deflection (cm)		
	u (8; 0)	v (8; 0)	u (16; 0)
10	-2.4377	-5.2398	-4.8751
20	-2.4371	-5.2215	-4.8742
30	-2.4371	-5.2181	-4.8740
40	-2.4369	-5.2168	-4.8740
50	-2.4370	-5.2164	-4.8740
60	-2.4370	-5.2161	-4.8740
70	-2.4370	-5.2159	-4.8739
75	-2.4370	-5.2159	-4.8739
80	-2.4370	-5.2159	-4.8739
100	-2.4370	-5.2159	-4.8739

(a)   (b)
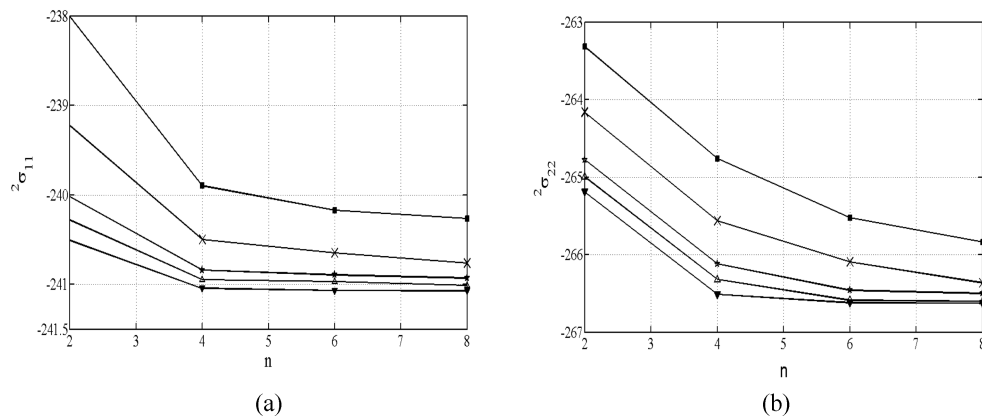
Fig. 3 Convergence analysis for (a) $^2\sigma_{11}$ ($L/2$, $h/2$), (b) $^2\sigma_{22}$ ($L/2$, $h/2$) for various values of m and n
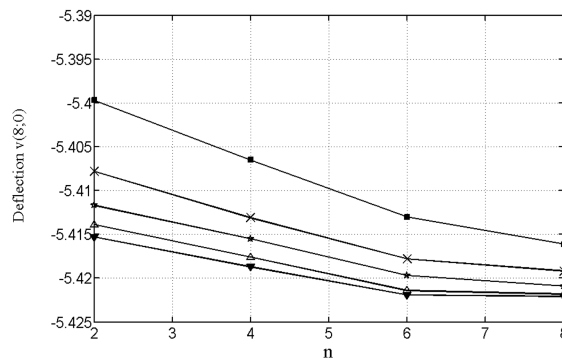
■ $m = 15$; ✕ $m = 20$; ☆ $m = 25$; △ $m = 30$; ▼ $m = 35$

Fig. 4 Convergence analysis for v ($L/2$, $h/2$) for various values of m and n

■ $m = 15$; ✕ $m = 20$; ☆ $m = 25$; △ $m = 30$; ▼ $m = 35$
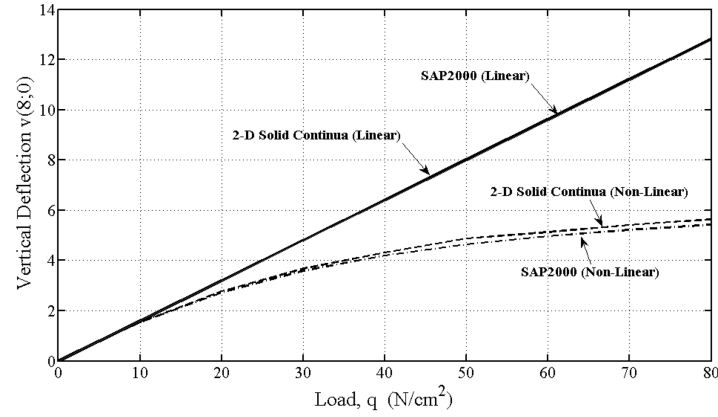
(a)
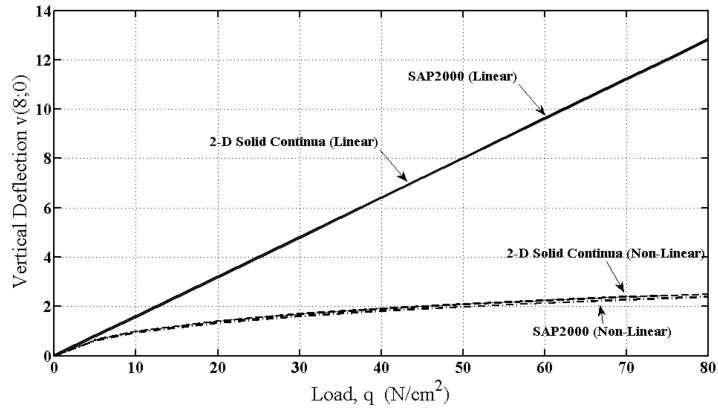
(b)

Fig. 5 Vertical displacement at $^0x_1 = 8$ cm, $^0x_1 = 0$-load curve for geometrically linear and geometrically nonlinear cases for $q = 70$ N/cm^2, $L = 16$ cm, $h = 2$ cm, $m = 35$, $n = 6$, for (a) pinned-rolled beam, (b) pinned-pinned beam

Increase in load is more effective in the vertical displacements of the linear solution. This situation may be explained as follows: In the linear case, arm of the external forces or arm of the external resultant force do not change with the magnitude of the external forces, and therefore the displacements depend on the external forces linearly. However, in the case of nonlinear analysis, the arm of the external forces change with the magnitude of the external force and, as the magnitude of the force increases the arm of these external forces decrease. However, as the forces increase the configuration of the beam become close to vertical direction and therefore increase in the load does not cause a significant increase in displacements after certain load level in which the configuration of the beam is close to the vertical direction. This situation is seen in Fig. 6 and Fig. 7 which shows the displaced configuration of the beam. After this load, it is expected that axial rigidity of the beam gains more importance than its flexural rigidity.

In the geometrically linear analysis, when there is no horizontal component of external loads affecting on the beam, namely when the external loads are perpendicular to the beam axis, the
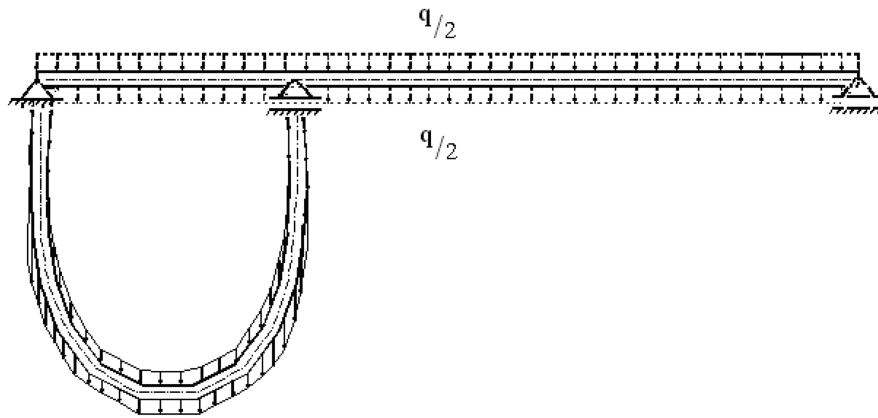
Fig. 6(a) Displaced configuration for $q = 20$ N/cm^2, $L = 50$ cm, $h = 2$ cm for pinned-rolled beam
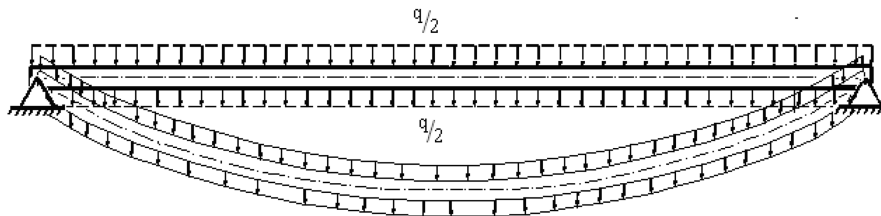
Fig. 6(b) Displaced configuration for $q = 20$ N/cm^2, $L = 50$ cm, $h = 2$ cm for pinned-pinned beam

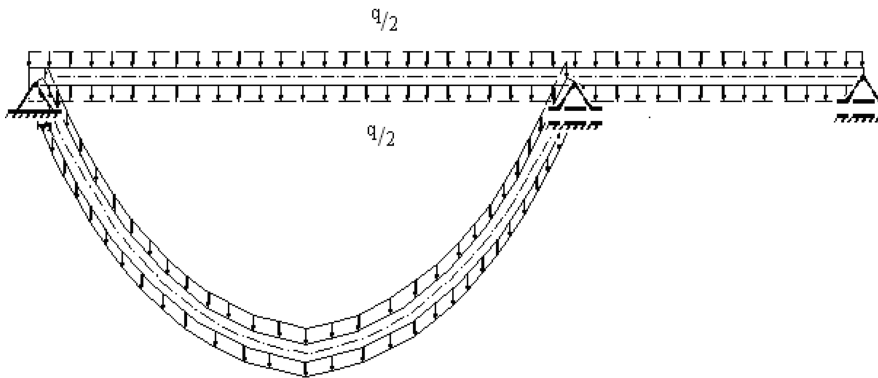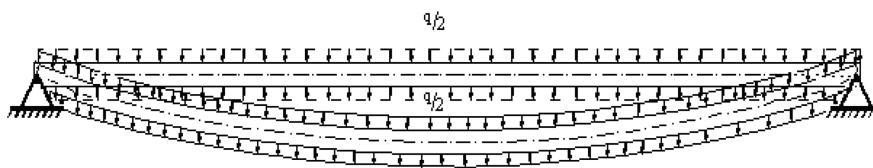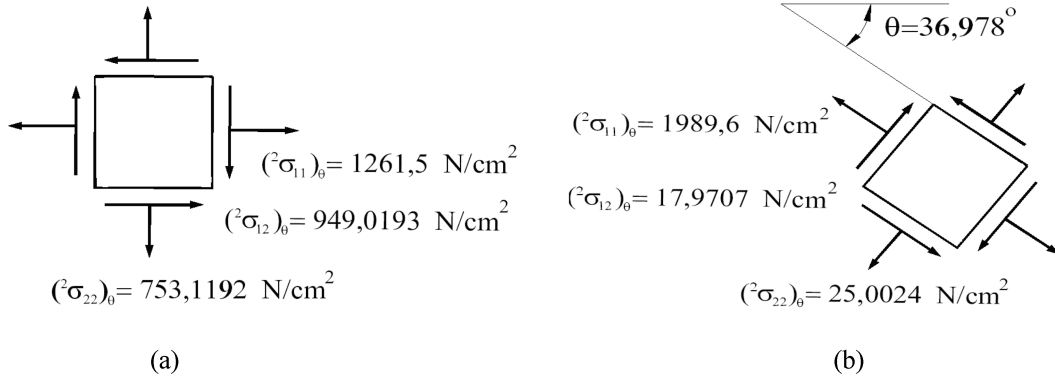Fig. 7(a) Displaced configuration for $q = 3$ N/cm^2, $L = 50$ cm, $h = 2$ cm for pinned-rolled beam

Fig. 7(b) Displaced configuration for $q = 3$ N/cm^2, $L = 50$ cm, $h = 2$ cm for pinned-pinned beam

Fig. 8 Stress state for pinned-rolled beam at (a) $^0x_1 = 16/3$ cm and $^0x_2 = -1$ cm, (b) stress state for rotated element corresponding to $^0x_1 = 16/3$ cm and $^0x_2 = -1$ cm

normal stress component $^0\sigma_{11}$ of stress tensor is zero at $^0x_2 = 0$ along the $^0x_1$ axis and then the $^0x_1$ axis is called as neutral axis. Because the equilibrium equations are written with respect to the initial configuration in which there is no displacement. However, in the geometrically nonlinear case, while the deflections occur, the non-follower external forces considered in this study do not remain perpendicular to the axis of the beam. This situation can be observed from Figs. 6 and 7.

The boundary conditions in the geometrically linear case are satisfied perfectly: Because in the present analysis, for $L = 16$ cm, $h = 2$ cm, $m = 35$ and $n = 6$, when $q = 70$ N/cm^2, $^0\sigma_{22} = 34.98$ N/cm^2 ≈ 35 N/cm^2. Now, the satisfaction of the boundary conditions in the geometrically nonlinear case will be investigated. For pinned-rolled beam, the angle between the tangent direction of any point of the upper or lower face after deformation of the beam and horizontal direction before deformation can be obtained by using Eq. (26). For $q = 70$ N/cm^2, for $^0x_1 = 16/3$ cm and $^0x_2 = -1$ cm, by using Eq. (26), the components of the line $d\mathbf{l}$ (consisting of the same material as $d\mathbf{L}$) after deformation in the horizontal and vertical directions which was the horizontal unit material line $d\mathbf{L}$ before deformation are obtained as 0.9420 in the horizontal direction and −0.7093 in the vertical direction for the beam shown in Fig. 1(a). By using these quantities, tangent of the line is −0.7093/0.9420 and therefore the angle between the tangent direction of the related point of the upper face and the horizontal direction is 36.978°.

The components $^2\sigma_{11} = 1261.5$ N/cm^2, $^2\sigma_{22} = 753.1192$ N/cm^2, $^2\sigma_{12} = -949.0193$ N/cm^2 of the stress tensor for the element shown in Fig. 8(a) in the considered location are found from the analysis and now it is desired to find the components of the stress tensor for the element shown in Fig. 8(b) of the same location by using the stress transformation equations for plane stress state

$$\left(^2\sigma_{11}\right)_\theta = \frac{^2\sigma_{11} + ^2\sigma_{22}}{2} + \frac{^2\sigma_{11} - ^2\sigma_{22}}{2}\cos 2\theta + {}^2\sigma_{12}\sin 2\theta = 1989.6 \text{ N/cm}^2 \tag{29}$$

$$\left(^2\sigma_{22}\right)_\theta = \frac{^2\sigma_{11} + ^2\sigma_{22}}{2} + \frac{^2\sigma_{11} - ^2\sigma_{22}}{2}\cos 2(\theta + 90) + {}^2\sigma_{12}\sin 2(\theta + 90) = 25.0024 \text{ N/cm}^2 \tag{30}$$

$$\left(^2\sigma_{12}\right)_\theta = -\frac{^2\sigma_{11} - ^2\sigma_{22}}{2}\sin 2\theta + {}^2\sigma_{12}\cos 2\theta = -17.9707 \text{ N/cm}^2 \tag{31}$$

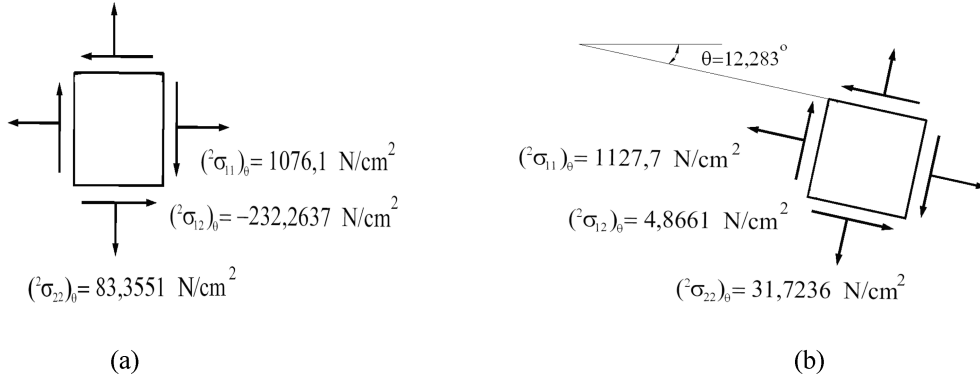(a)   (b)

Fig. 9 Stress state for pinned-pinned beam at (a) $^0x_1 = 16/3$ cm and $^0x_2 = -1$ cm, (b) stress state for rotated element corresponding to $^0x_1 = 16/3$ cm and $^0x_2 = -1$ cm

From these equations $(^2\sigma_{11})_\theta = 1989.6$ N/cm^2, $(^2\sigma_{22})_\theta = 25.0024$ N/cm^2 and $(^2\sigma_{12})_\theta = -17.9707$ N/cm^2. These values show that the boundary conditions are satisfied in the nonlinear case. Because

$$dL = 1.00 \text{ cm} \rightarrow dl = 1.1363 \text{ cm}$$

$$\sqrt{(^2\sigma_{22})_\theta^2 + (^2\sigma_{12})_\theta^2} = 30.7907 \text{ N/cm}^2 \cong 35/dl = 30.8017 \text{ N/cm}^2 \tag{32}$$

For pinned-pinned beam, the angle between the tangent direction of any point of the upper or lower face after deformation of the beam and horizontal direction before deformation can be obtained by using Eq. (26). For $q = 70$ N/cm^2, for $^0x_1 = 16/3$ cm and $^0x_2 = -1$ cm, by using Eq. (26), the components of the line $d\mathbf{l}$ (consisting of the same material as $d\mathbf{L}$) after deformation in the horizontal and vertical directions which was the horizontal unit material line $d\mathbf{L}$ before deformation are obtained as 1.0871 in the horizontal direction and -0.2367 in the vertical direction for the beam shown in Fig. 1(b). By using these quantities, tangent of the line is $-0.2367/1.0871$ and therefore the angle between the tangent direction of the related point of the upper face and the horizontal direction is 12.2836°.

The components $^2\sigma_{11} = 1076,1$ N/cm^2, $^2\sigma_{22} = 83,3551$ N/cm^2, $^2\sigma_{12} = -232,263$ N/cm^2 of the stress tensor for the element shown in Fig. 9(a) in the considered location are found from the analysis and now it is desired to find the components of the stress tensor for the element shown in Fig. 9(b) of the same location by using the stress transformation equations for plane stress state

$$(^2\sigma_{11})_\theta = \frac{^2\sigma_{11} + {}^2\sigma_{22}}{2} + \frac{^2\sigma_{11} - {}^2\sigma_{22}}{2}\cos 2\theta + {}^2\sigma_{12}\sin 2\theta = 1127,7 \text{ N/cm}^2 \tag{33}$$

$$(^2\sigma_{22})_\theta = \frac{^2\sigma_{11} + {}^2\sigma_{22}}{2} + \frac{^2\sigma_{11} - {}^2\sigma_{22}}{2}\cos 2(\theta + 90) + {}^2\sigma_{12}\sin 2(\theta + 90) = 31,7236 \text{ N/cm}^2 \tag{34}$$

$$(^2\sigma_{12})_\theta = -\frac{^2\sigma_{11} - {}^2\sigma_{22}}{2}\sin 2\theta + {}^2\sigma_{12}\cos 2\theta = -4,8661 \text{ N/cm}^2 \tag{35}$$

From these equations $(^2\sigma_{11})_\theta = 1127,7$ N/cm^2, $(^2\sigma_{22})_\theta = 31,7236$ N/cm^2 and $(^2\sigma_{12})_\theta = -4,8661$ N/cm^2. These values show that the boundary conditions are satisfied in the nonlinear case. Because

$$dL = 1.00 \text{ cm} \rightarrow dl = 1.0904 \text{ cm}$$

$$\sqrt{\left(^2\sigma_{22}\right)_\theta^2 + \left(^2\sigma_{12}\right)_\theta^2} = 32{,}0946 \text{ N/cm}^2 \cong 35/dl = 32{,}0979 \text{ N/cm}^2 \tag{36}$$

By using Eq. (8), the support reactions are obtained in nodes of related finite elements. The $A_{0_{x_1}}$ and $A_{0_{x_2}}$ values given in Tables 2 and 3 are support reactions at the end A in the $^0x_1$ and $^0x_2$ respectively, The $B_{0_{x_1}}$ and $B_{0_{x_2}}$ values given in Tables 2 and 3 are support reactions at the end B in the $^0x_1$ and $^0x_2$ respectively.

In Table 4, very great values of loads are used for obtaining displacements close to $L/2$. It is seen from Table 4 that the difference between the results of two dimensional solid continuum (2DSC) and SAP2000 which uses Timoshenko beam theory increases with decrease in the length of the beam. It can be said that when the ratio L/h is approximately equal or greater than 8, then both of the finite element model of two dimensional continuum and the SAP2000 can be used to analyze the problem in the geometrically linear case. However, in the geometrically nonlinear case, for the difference ratio ((2DSC-SAP2000)/2DSC) lower then 1%, L/h ratio must be equal or greater than 25.

It is known that in the failure analysis, the most important quantities are the principal normal stresses $^2\sigma_{max}$, $^2\sigma_{min}$ and the maximum shear stress $^2\sigma_{12max}$

$$^2\sigma_{max} = \frac{^2\sigma_{11} + ^2\sigma_{22}}{2} + \sqrt{\left(\frac{^2\sigma_{11} - ^2\sigma_{22}}{2}\right)^2 + \left(^2\sigma_{12}\right)^2} \tag{37}$$

$$^2\sigma_{min} = \frac{^2\sigma_{11} + ^2\sigma_{22}}{2} - \sqrt{\left(\frac{^2\sigma_{11} - ^2\sigma_{22}}{2}\right)^2 + \left(^2\sigma_{12}\right)^2} \tag{38}$$

$$^2\sigma_{12max} = \frac{^2\sigma_{max} + ^2\sigma_{min}}{2} \tag{39}$$

Table 2 Displacements and support reactions for pinned-rolled beam for $L = 16$ cm, $h = 2$ cm

q (N/cm²)	u (8; 0) (cm)	v (8; 0) (cm)	$A_{0_{x_1}}$ (N)	$A_{0_{x_2}}$ (N)	$B_{0_{x_2}}$ (N)
10	-0.3682	-1.5364	0	80.00	80.00
20	-0.6190	-2.7769	0	160.00	160.00
30	-1.1209	-3.6745	0	240.00	240.00
50	-2.0073	-4.8714	0	400.00	400.00
70	-2.6710	-5.4219	0	560.00	560.00

Table 3 Displacements and support reactions for pinned-pinned beam for $L = 16$ cm, $h = 2$ cm

q (N/cm²)	u (8; 0) (cm)	v (8; 0) (cm)	$A_{0_{x_1}}$ (N)	$B_{0_{x_1}}$ (N)	$A_{0_{x_2}}$ (N)	$B_{0_{x_2}}$ (N)
10	0	-0.9923	120.4108	120.4108	80.00	80.00
20	0	-1.4145	248.2611	248.2611	160.00	160.00
30	0	-1.6952	359.4557	359.4557	240.00	240.00
50	0	-2.0904	552.8717	552.8717	400.00	400.00
70	0	-2.3947	720.4720	720.4720	560.00	560.00

Table 4 Displacements for pinned-rolled beam for various lengths of beam

$L/h = 8$ $q = 70$ N/cm^2 ($L = 16$ cm, $h = 2$ cm)					
(cm)	2-D ($m = 35, n = 6$)		Sap 2000 ($m = 70$)		Diffirence % $= \left(\dfrac{2DSC - SAP2000}{2DSC} \right) \times 100$	
	Linear	Non-linear	Linear	Non-linear	Linear	Non-linear
u (8; 0)	0.00	-2.6710	0.00	-2.437	-	8.761
v (8; 0)	-11.2076	-5.4219	-11.1838	-5.2173	0.212	3.773
u (16; 0)	0.00	-5.3420	0.00	-4.874	-	8.761
$L/h = 10$ $q = 50$ N/cm^2 ($L = 20$ cm, $h = 2$ cm)					
(cm)	2-D ($m = 35, n = 6$)		Sap 2000 ($m = 70$)		Diffirence % $= \left(\dfrac{2DSC - SAP2000}{2DSC} \right) \times 100$	
	Linear	Non-linear	Linear	Non-linear	Linear	Non-linear
u (10; 0)	0.00	-4.0024	0.00	-3.7641	-	5.953
v (10; 0)	-19.2717	-7.2047	-19.259	-7.0404	0.065	2.280
u (20; 0)	0.00	-8.0049	0.00	-7.5283	-	5.953
$L/h = 15$ $q = 20$ N/cm^2 ($L = 30$ cm, $h = 2$ cm)					
(cm)	2-D ($m = 35, n = 6$)		Sap 2000 ($m = 70$)		Diffirence % $= \left(\dfrac{2DSC - SAP2000}{2DSC} \right) \times 100$	
	Linear	Non-linear	Linear	Non-linear	Linear	Non-linear
u (15; 0)	0.00	-6.7492	0.00	-6.5664	-	2.708
v (15; 0)	-38.5173	-11.1495	-38.511	-11.0474	0.016	0.915
u (30; 0)	0.00	-13.4985	0.00	-13.1327	-	2.708
$L/h = 20$ $q = 10$ N/cm^2 ($L = 40$ cm, $h = 2$ cm)					
(cm)	2-D ($m = 35, n = 6$)		Sap 2000 ($m = 70$)		Diffirence % $= \left(\dfrac{2DSC - SAP2000}{2DSC} \right) \times 100$	
	Linear	Non-linear	Linear	Non-linear	Linear	Non-linear
u (20; 0)	0.00	-9.5529	0.00	-9.4092	-	1.504
v (20; 0)	-60.5891	-15.1074	-60.588	-15.0558	0.0018	0.342
u (40; 0)	0.00	-19.1059	0.00	-18.8184	-	1.504
$L/h = 25$ $q = 5$ N/cm^2 ($L = 50$ cm, $h = 2$ cm)					
(cm)	2-D ($m = 35, n = 6$)		Sap 2000 ($m = 70$)		Diffirence % $= \left(\dfrac{2DSC - SAP2000}{2DSC} \right) \times 100$	
	Linear	Non-linear	Linear	Non-linear	Linear	Non-linear
u (25; 0)	0.00	-11.7637	0.00	-11.6477	-	0.986
v (25; 0)	-73.808	-18.7235	-73.807	-18.6741	0.0014	0.263
u (50; 0)	0.00	-23.5275	0.00	-23.2953	-	0.986

An eight-node quadratic element was used by Reddy (2004) to solve an uniformly loaded cantilever beam: It was noted by Reddy (2004) that the stresses could not be obtained truly apart from the Gauss points. Also, it is found by us that the boundary conditions at the free surfaces of the beam cannot be satisfied in the eight-node quadratic element. Therefore, a twelve-node quadratic element is used in this study instead of eight-node quadratic element and as shown above, boundary conditions at the free surfaces are satisfied perfectly. Also, it will be shown in the following figures that the stresses are obtained truly everywhere on the cross section.

The stress diagrams at $^0x_1 = 8$ cm along the $^0x_2$ axis are given in Figs. 10-17 for geometrically nonlinear and linear cases for $q = 70$ N/cm^2, $L = 16$ cm, $h = 2$ cm. In Figs. 10, 11, the stress distributions for geometrically linear case is denoted by $^0\sigma_{11}$, $^0\sigma_{22}$, the Cauchy stress distributions is denoted by $^2\sigma_{11}$, $^2\sigma_{22}$ and the second Piola-Kirchhoff stress tensor is denoted by $^2_0S_{11}$, $^2_0S_{22}$ for
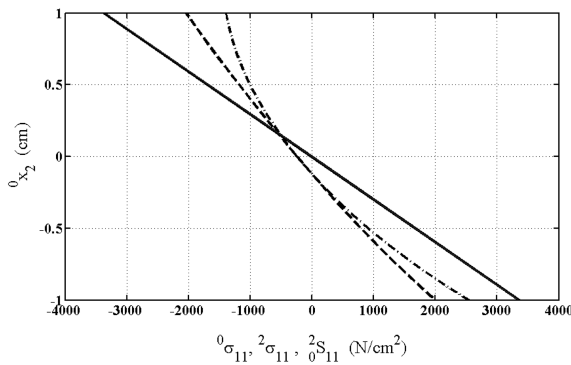

Fig. 10 Normal stresses for the cross section at $^0x_1 = 8$ cm for the pinned-rolled beam for $q = 70$ N/cm^2, $L = 16$ cm, $m = 35$, $n = 6$, $^0\sigma_{11}$ (——); $^2\sigma_{11}$ (—·—·—); $^2_0S_{11}$ (– – –)
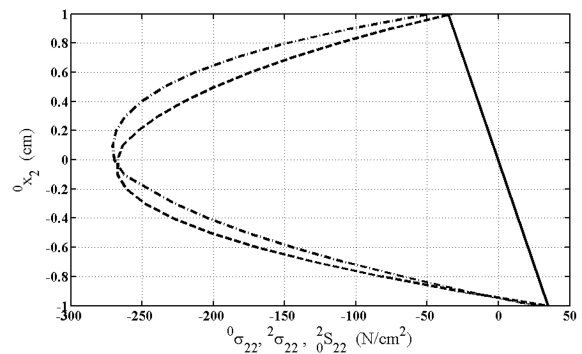

Fig. 11 Normal stresses for the cross section at $^0x_1 = 8$ cm for the pinned-rolled beam for $q = 70$ N/cm^2, $L = 16$ cm, $h = 2$ cm, $m = 35$, $n = 6$, $^0\sigma_{22}$ (——); $^2\sigma_{22}$ (—·—·—); $^2_0S_{22}$ (– – –)
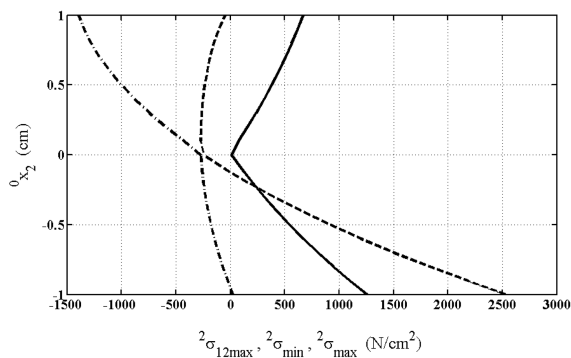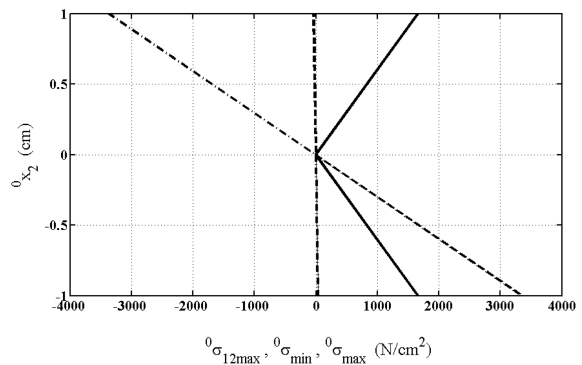

Fig. 12 The principal stresses $^2\sigma_{min}$, $^2\sigma_{max}$ and maximum shear stress $^2\sigma_{12max}$ at $^0x_1 = 8$ cm for the pinned-rolled beam for $q = 70$ N/cm^2, $L = 16$ cm, $h = 2$ cm, $m = 35$, $n = 6$ in the geometrically non-linear case, $^2\sigma_{12max}$ (——); $^2\sigma_{min}$ (—·—·—); $^2\sigma_{max}$ (– – –)

Fig. 13 The principal stresses $^0\sigma_{min}$, $^0\sigma_{max}$ and maximum shear stress $^0\sigma_{12max}$ at $^0x_1 = 8$ cm for the pinned-rolled beam for $q = 70$ N/cm^2, $L = 16$ cm, $h = 2$ cm, $m = 35$, $n = 6$ in the geometrically linear case, $^0\sigma_{12max}$ (——); $^0\sigma_{min}$ (—·—·—); $^0\sigma_{max}$ (– – –)
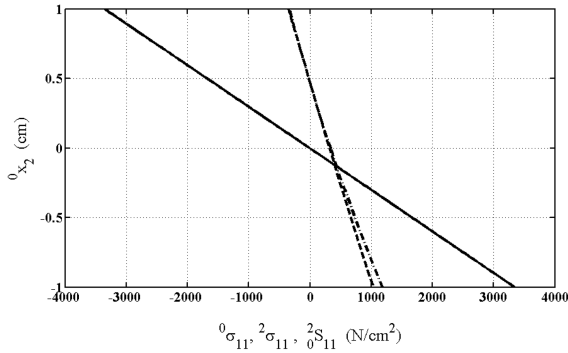
Fig. 14 Normal stresses for the cross section at $^{0}x_1 = 8$ cm for the pinned- pinned beam for $q = 70$ N/cm^2, $L = 16$ cm, $h = 2$ cm, $m = 35$, $n = 6$, $^{0}\sigma_{11}$ (——); $^{2}\sigma_{11}$ (–·–·–); $^{2}_{0}S_{11}$ (– – –)
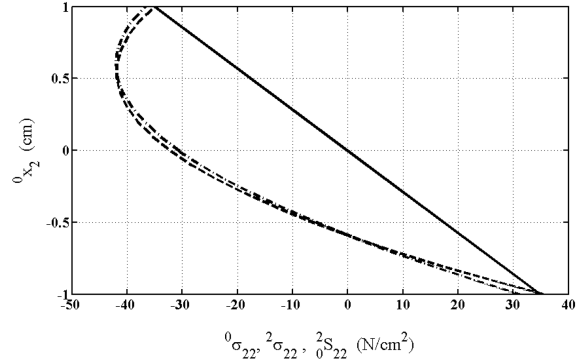

Fig. 15 Normal stresses for the cross section at $^{0}x_1 = 8$ cm for the pinned- pinned beam for $q = 70$ N/cm^2, $L = 16$ cm, $h = 2$ cm, $m = 35$, $n = 6$, $^{0}\sigma_{22}$ (——); $^{2}\sigma_{22}$ (–·–·–); $^{2}_{0}S_{22}$ (– – –)

Fig. 16 The principal stresses $^{2}\sigma_{min}$, $^{2}\sigma_{max}$ and maximum shear stress $^{2}\sigma_{12max}$ at $^{0}x_1 = 8$ cm for the pinned- pinned beam for $q = 70$ N/cm^2, $L = 16$ cm, $h = 2$ cm, $m = 35$, $n = 6$ in the geometrically non-linear case, $^{2}\sigma_{12max}$ (——); $^{2}\sigma_{min}$ (–·–·–); $^{2}\sigma_{max}$ (– – –)
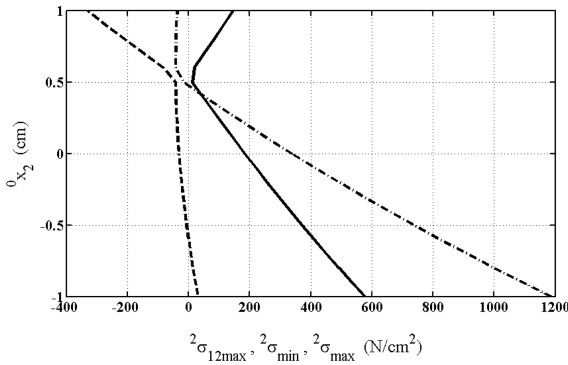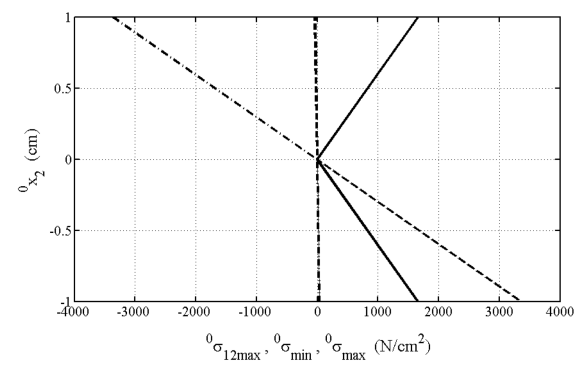

Fig. 17 The principal stresses $^{0}\sigma_{min}$, $^{0}\sigma_{max}$ and maximum shear stress $^{0}\sigma_{12max}$ at $^{0}x_1 = 8$ cm for the pinned- pinned beam for $q = 70$ N/cm^2, $L = 16$ cm, $h = 2$ cm, $m = 35$, $n = 6$ in the geometrically linear case, $^{0}\sigma_{12max}$ (——); $^{0}\sigma_{min}$ (–·–·–); $^{0}\sigma_{max}$ (– – –)

$q = 70$ N/cm^2, $m = 35$, $n = 6$.

The principal normal stresses $^{2}\sigma_{max}$, $^{2}\sigma_{min}$ and the maximum shear stress $^{2}\sigma_{12max}$ distributions for the geometrically nonlinear case are given in Fig. 12. The principal normal stresses $^{0}\sigma_{max}$, $^{0}\sigma_{min}$ and the maximum shear stress $^{0}\sigma_{12max}$ distributions for the geometrically linear case are given in Fig. 13. It is seen from Figs. 12 and 13 that the principal normal stresses and the maximum shear stress obtained in the geometrically linear case are very greater than the principal normal stresses and the maximum shear stress obtained in the geometrically nonlinear case. In Figs. 14-17, the similar diagrams to the diagrams given by Figs. 10-13 for the pinned-rolled beam are given for the pinned-pinned beam. Again, it is seen from Figs. 16 and 17 that the principal normal stresses and the maximum shear stress obtained in the geometrically linear case are very greater than the principal normal stresses and maximum shear stress obtained in the geometrically nonlinear case. It can be

observed from Figs. 12 and 16 that the principal normal stresses and the maximum shear stress obtained in the pinned-rolled beam are very greater than the principal normal stresses and maximum shear stress obtained in the pinned-pinned beam for geometrically nonlinear case.

4. Conclusions

The geometrically non-linear static responses of a cantilevered beam made of hyperelastic material subjected to a non-follower transversal uniformly distributed load has been studied. In the study, the finite element model of the beam is constructed by using total Lagrangian finite element model of two dimensional continuum for a twelve-node quadratic element. The considered highly non-linear problem is solved by using incremental displacement-based finite element method in conjunction with Newton-Raphson iteration method. There is no restriction on the displacements. The effects of the geometric non-linearity and pinned-pinned and pinned-rolled support conditions on the displacements and on the stresses are investigated. The comparison and the convergence studies are performed. By using a twelve-node quadratic element, the free boundary conditions are satisfied perfectly which are not satisfied before in other studies and very good stress diagrams are obtained which are not obtained for two-dimensional continuum models of geometrically non linear analyses of beams. It is known that in the failure analysis, the most important quantities are the principal normal stresses and the maximum shear stress. Therefore, these stresses are investigated and shown by figures in detail which are very different from the related stresses of geometrically linear case.

It is observed from the investigations that geometrical non-linearity and pinned-pinned and pinned-rolled support conditions play very important role on the responses of the beam as the displacements increase. In fact, as it is known, after some values of displacements which can be determined according to the parameters of the problem, it is inevitable to analyze the problem as geometrically non-linear. Also, it is seen from the investigations that the difference between the results of finite element model of two dimensional solid continuum and SAP2000 which uses Timoshenko beam theory increases considerably in the geometrically nonlinear case while the beam length/beam height ratio decreases Therefore, for small ratios of beam length/beam height, finite element model of two dimensional solid continuum must be used instead of SAP2000 which uses Timoshenko beam theory.

References

Akbaş, Ş.D. and Kocatürk, T. (2009), "Geometrically non-linear static analysis of simply supported beams made of hyperelastic material", *XVI. Turkish National Mechanic Congress,* Kayseri, Turkey, 115-125 (in Turkish).

Al-Sadder, A. and Al-Rawi, R.A.O. (2006), "Finite difference scheme for large-deflection analysis of non-prismatic cantilever beams subjected to different types of continuous and discontinuous loadings", *Arch. Appl. Mech.*, **75**(8-9), 459-473.

Al-Sadder, S.Z., Othman, R.A. and Shatnawi, A.S. (2006), "A simple finite element formulation for large deflection analysis of nonprismatic slender beams", *Struct. Eng. Mech.*, **24**(6), 647-664.

Chucheepsakul, S., Buncharoen, S. and Huang, T. (1995), "Elastica of a simple variable-arc-length beam subjected to an end moment", *J. Eng. Mech.-ASCE*, **121**(7), 767-772.

Chucheepsakul, S., Buncharoen, S. and Wang, C.M. (1994), "Large deflection of beams under moment gradient", *J. Eng. Mech.-ASCE*, **120**(9), 1848-1860.

CSI Computers & Structures Inc. (2009), SAP2000-Version 14 Three Dimensional Static and Dynamic Finite

Element Analysis and Design of Structures, Berkeley, Computers & Structures Inc.

He, X.Q., Wang, C.M. and Lam, K.Y. (1997), "Analytical bending solutions of elastica with one end held while the other end portion slides on a friction support", *Arch. Appl. Mech.*, **67**(8), 543-554.

Kapania, R.K. and Li, J.A. (2003), "A formulation and implementation of geometrically exact curved beam elements incorporating finite strains and finite rotations", *Comput. Mech.*, **30**(5-6), 444-459.

Li, S.R. and Zhou, Y.H. (2005), "Post-buckling of a hinged-fixed beam under uniformly distributed follower forces", *Mech. Res. Commun.*, **32**, 359-367.

Pulngern, T., Chucheepsakul, S. and Halling, M.W. (2005), "Large deflections of variable-arc-length beams under uniform self weight: Analytical and experimental", *Struct. Eng. Mech.* **19**(4), 413-423.

Reddy, J.N. (2004), *An Introduction to Non-linear Finite Element Analysis*, Oxford University Press Inc.

Wang, C.M., Lam, K.Y., He, X.Q. and Chucheepsakul, S. (1997), "Large deflections of an end supported beam subjected to a point load", *Int. J. Nonlin. Mech.*, **32**(1), 63-72.

Zienkiewichz, O.C. and Taylor, R.L. (2000), *The Finite Element Method*, Fifth Edition, Volume 2: Solid Mechanics, Oxford: Butterworth-Heinemann.